Ab initio study of the ground state properties of molecular oxygen

ARTICLE *in* SPECTROCHIMICA ACTA PART A MOLECULAR AND BIOMOLECULAR SPECTROSCOPY · MAY 2004

Impact Factor: 2.35 · DOI: 10.1016/S1386-1425(03)00334-2 · Source: PubMed

1 AUTHOR:

Boris Minaev
Черкаський національний університ...

323 PUBLICATIONS **3,122** CITATIONS

SEE PROFILE

Available online at www.sciencedirect.com
SCIENCE DIRECT®
Spectrochimica Acta Part A 60 (2004) 1027–1041
SPECTROCHIMICA ACTA PART A
www.elsevier.com/locate/saa

Ab initio study of the ground state properties of molecular oxygen

Boris F. Minaev [a,b,*]

[a] *Department of Chemistry, State University of Technology, Cherkassy 18006, Ukraine*
[b] *Laboratory of Theoretical Chemistry, SCFAB, The Royal Institute of Technology, SE-10691 Stockholm, Sweden*

Received 13 May 2003; received in revised form 7 July 2003; accepted 7 July 2003

Abstract

The electric and magnetic properties of the ground state of oxygen molecule are calculated by multiconfiguration self-consisted field (MCSCF) method and compared with experimental data: the quadrupole moment, polarizability, the ^{17}O nuclear quadrupole coupling constant, magnetizability tensor, nuclear spin–rotation coupling constant and rotational *g* factor. The last two constants are calculated for all possible isotope modifications. The rotational, ESR and NMR spectra are discussed. Fermi-contact hyperfine coupling parameter is additionally estimated by different methods. The NMR chemical shielding tensor for $^{17}O^{16}O$ species at high temperature limit (without electron spin contribution) is predicted. Potential energy curves for 10 excited bound states and the internuclear distance dependence of the studied properties are also presented.

Keywords: Dioxygen; Quadrupole moment; Polarizability; Magnetic properties; Hyperfine coupling constants; ESR and NMR spectra

1. Introduction

Dioxygen molecule is one of the most abundant and the most important species in biosphere of the Earth. O_2 is used as an oxidant in respiration of mammals and in oxidative metabolic processes, reducing food to water and carbon dioxide. These reactions are equivalent to combustion by their exothermicity. But living cells smoothly release energy in soft conditions, whereas combustion is a radical chain process connected with high temperature initiation and proceeding [1–4]. These peculiarities are determined by the triplet nature of the ground state of the O_2 molecule. Since Faraday's discovery of paramagnetism of molecular oxygen, the connection between spin nature of the O_2 molecule, its sluggish reactivity at room temperature and O_2 involvement in bioprocesses are still not completely understood [1,5]. Life strongly depends on the kinetic barriers of molecular oxygen reactions, which are determined by spin restrictions; direct insertion of O_2 into diamagnetic molecules is forbidden by spin selection rules. During interaction with a diamagnetic reagent the spin density from O_2 penetrates to the reagent and produces paramagnetic NMR chemical shift [2,6]; this makes easier spin uncoupling inside diamagnetic species. Recently [7], oxygen is used as a paramagnetic probe of membrane protein structure studied by NMR method. Spin-forbidness of diamagnetic oxidative product release can be overcome by exchange interactions with paramagnetic metal centre of the mono-oxygenase enzymes or by spin–orbit coupling effects [5,8].

That is why it is important to know as much as possible about the magnetic and electric properties of the ground state of the O_2 molecule. Polarizability [9], quadrupole moments [10], magnetizability [11,12], the ^{17}O nuclear quadrupole coupling (NQC) constant [13] and other ESR parameters [13–16] are known for the O_2 ground state from experiment. The NMR spectrum of the oxygen molecule has not been measured so far. The paramagnetism of the O_2 molecule and quadrupole moment of the active ^{17}O nuclei leads to a fast spin relaxation and a very wide NMR signal, which is difficult to observe. But the NMR spectrum could be measured (in principle) in a diamagnetic α-oxygen crystal. The internuclear distance dependence of all these parameters can be used as an important criterion of oxygen reactivity.

Though O_2 has no electric dipole moment, the microwave spectrum is observed being induced by magnetic dipole transitions. The microwave absorption spectrum of the $^{16}O^{17}O$ isotope species shows a rich hyperfine structure arising from magnetic dipole and electric quadrupole interactions of the

* Tel.: +46-8-5537-8417; fax: +46-8-5537-8590.
E-mail address: boris@theochem.kth.se (B.F. Minaev).

1386-1425/$ – see front matter © 2003 Elsevier B.V. All rights reserved.
doi:10.1016/S1386-1425(03)00334-2

^{17}O nuclear spin with the unpaired electron spins [13–15]. The theory of the hyperfine structure is given by Frosch and Foley [17] and the observed microwave spectrum fits it well [14]. The hyperfine structure of the ESR spectrum of gaseous $^{16}O^{17}O$ has been interpreted with account of the ^{17}O nuclear quadrupole coupling constant and the nuclear spin–rotation coupling (NSRC) constant [13]. The hyperfine coupling (HFC) constants of the spin-Hamiltonian were interpreted by simple MO models [13–15] and also by ab initio configuration interaction (CI) calculation with a minimal basis set [18].

Magnetizability tensor, nuclear spin–rotation coupling constant and rotational g factor are also important parameters for molecular Zeeman effect, Cotton–Mouton effect and microwave spectrum interpretation [11,13,16]. Polarizability and quadrupole moment can be used for the intermolecular interaction analysis and for the solvent shift estimations. These properties are very sensitive to the quality of the wave function and have been calculated by many authors [9,18–20].

The ESR fine-structure parameters of the ground state connected with the electron spin and spin–orbit coupling perturbation (effective spin–spin coupling constant λ, electronic g factor and electronic spin–rotation coupling constant γ) [21] have been calculated before by semi-empirical INDO-type CI method [2,22–24] and by ab initio methods (λ_e) [25–27], including the multiconfiguration self-consisted field (MCSCF) response technique (g factor and γ constant) [28–30]. These electronic spin parameters are not considered here. Other electric and magnetic properties are calculated and discussed later.

2. Method of calculations

MCSCF method is a general basis [31] for the present approach. The MCSCF calculations of O_2 molecule have been performed with different complete active spaces (CAS). They include different numbers of active electrons (N) and occupied MOs of the ground configuration:

$$^3\psi_0[X^3\Sigma_g^-] = \mathcal{A}(1\sigma_g)^2(1\sigma_u)^2(2\sigma_g)^2(2\sigma_u)^2(3\sigma_g)^2(\pi_u)^4(\pi_g)^2, \quad (1)$$

where $\mathcal{A}$ indicates the anti-symmetrization product; the $3\sigma_u$, $4\sigma_{g,u}$ and $2\pi_{u,g}$ empty orbitals were also included in some CAS. Specification of different CAS used in the present work is given in Table 1. Two active spaces have been widely used before: CAS I ((2, 3)σ_u(3, 4)σ_g(1, 2)$\pi_u 1\pi_g$) and CAS II ((2, 3)σ_u(3, 4)σ_g(1, 2)π_u(1, 2)π_g) with 10 active electrons ($N = 10$) [32,33]. The total number of configuration state functions (CSFs) is 5588 and 35,440, respectively, in these

Table 1
Properties of the ground state of the oxygen molecule calculated by MCSCF method with the "aug-cc-pVTZ" basis sets and with different complete active spaces at the experimental equilibrium internuclear distance, $r_e = 1.207536$ Å [21]

i	CAS (N)	g_r[a]	Q_{zz}	χ_{xx}	χ_{zz}	α_{xx}	α_{zz}	V_{zz}	σ[b]
1	$3\sigma_g 3\sigma_u 1\pi_u 1\pi_g$ (8)	−0.201	−0.289	−1.613	−3.686	7.244	14.332	−7.925	−28.58
2	(2, 3)$\sigma_u 3\sigma_g 1\pi_u 1\pi_g$ (10)	−0.200	−0.288	−1.630	−3.684	7.227	14.445	−7.932	−24.51
3	(2, 3)$\sigma_u 3\sigma_g$(1, 2)$\pi_u 1\pi_g$ (10)	−0.180	−0.160	−1.823	−3.710	7.660	14.744	−8.078	−8.48
4	(2, 3)σ_g(2, 3)σ_u(1, 2)$\pi_u 1\pi_g$ (12)	−0.187	−0.117	−1.746	−3.711	8.208	14.575	−8.030	−16.45
5	$3\sigma_g 3\sigma_u$(1, 2)π_u(1, 2)π_g (8)	−0.219[a]	−0.176	−1.524	−3.746	7.787	14.934	−8.003	−36.10
6	(3, 4)σ_g(3, 4)σ_u(1, 2)π_u(1, 2)π_g (8)	−0.220[a]	−0.208	−1.523	−3.749	7.920	14.797	−8.065	−48.11
7	(2, 3)$\sigma_u 3\sigma_g$(1, 2)π_u(1, 2)π_g (10)	−0.204	−0.169	−1.609	−3.743	7.488	15.583	−8.000	−32.29
8	(2, 3)σ_g(2, 3)σ_u(1, 2)π_u(1, 2)π_g (12)	−0.228	−0.168	−1.358	−3.746	7.873	16.602	−7.963	−55.27
9	(2, 3)σ_u(3, 4)σ_g(1, 2)$\pi_u 1\pi_g$ (10)	−0.183	−0.105	−1.803	−3.720	7.708	14.526	−8.161	−9.01
10	(2, 3)σ_u(3, 4)σ_g(1, 2)π_u(1, 2)π_g (10)	−0.217	−0.177	−1.488	−3.757	6.513	15.414	−8.131	−37.74
11	(2–4)σ_g(2–4)σ_u(1, 2)π_u(1, 2)π_g (12)	−0.230[a]	−0.254	−1.464	−3.776	8.044	15.455	−8.154	−42.50
–	Experiment	−0.23[c]	−0.26[d]	−1.46[e]	−3.78[e]	8.16[f]	15.45[f]	−8.42 ± 0.2[g]	–

N is a number of active electrons, g_r the rotational g factor, Q_{zz} the electric quadrupole tensor component ($Q_{xx} = Q_{yy} = -(1/2)Q_{zz}$)($ea_0^2$), χ the temperature-independent magnetizability tensor, $\chi_{xx} = \chi_{yy}$ (a.u.) (1 a.u. = 4.75182 ppm cm^3 mol^{-1} (CGS units of magnetic susceptibility)), α the static polarizability (a.u.), V_{zz} the nuclear quadrupole coupling constant (MHz), σ the isotropic NMR shielding constant (ppm). V_{zz} and σ are calculated for $^{17}O_2$ isotope, g_r for $^{16}O^{17}O$ and $^{16}O_2$ isotopes

[a] This molecular rotational g_r factor is calculated for $^{16}O_2$ molecule; all others presented values correspond to the $^{16}O^{17}O$ isomer (the difference between two isotope modification is 2.3%).

[b] The temperature independent part of the isotropic shielding tensor.

[c] From [13,46]. This rotational g_r factor is expressed in m/M units. The electron/proton mass ratio $(m/M) = 0.000544$. In [13,16], the molecular rotational g factor is given in the form: $g_r = -(1.35 \pm 0.3) \times 10^{-4} = -(0.25 \pm 0.05)$. In [46], it is $g_r = -(1.25 \pm 0.08) \times 10^{-4}$, which corresponds to $-(0.23 \pm 0.01)(m/M)$.

[d] From [10].

[e] Estimated with account of anisotropy from [11]. Magnetizability is presented without spin contribution; this is temperature independent part of magnetic susceptibility.

[f] Frequency corrected values [9].

[g] From [13].

two CASs in the D_{2h} point group. For the spin–rotation coupling constant calculations, the non-symmetrical nuclei have to be considered, thus the C_{2v} point group has also been implemented (both nuclei are along the C_2 axis). In that case, the total number of configurations is 70,880 CSFs in the CAS II. These two active spaces are denoted as 9-CAS and 10-CAS in Table 1.

Other active spaces were also studied accounting the following arguments. The two inner MOs with the energy −20.8 a.u. were excluded from all CASs quite naturally; inclusion of other occupied MO was studied by analysis of calculated properties (Table 1). The simplest 1-CAS includes the most important $3\sigma_g 1\pi_u 1\pi_g 3\sigma_u$ orbitals, consisting mostly from the 2p-AOs. It is also called 2p-CAS and is sufficient for qualitatively correct studies [19,23]. Other CASs include addition of the $2\sigma_u$-MO, which is close in energy. The previous experience [33,34] indicates that the inclusion of the $2\pi_{u,g}$, $4\sigma_{g,u}$ empty orbitals is very desirable. The largest active space, 11-CAS (Table 1), includes addition of the strongly bonding $2\sigma_g$-MO; this CAS consists of a half million configuration state functions (12 electrons in 14 MOs). This well-balanced CAS is the only one, which describes all properties pretty well.

The correlation consistent basis of Woon and Dunning augmented by polarization functions, aug-cc-pVTZ [35], which contains 116 primitives and 92 contracted atomic orbitals for molecular oxygen, is used. The London atomic orbitals are used to ensure gauge-origin independent results [36]. For calculation of the HFC constants other basis sets and the MCSCF technique, described in [37], are implemented. The uncontracted aug-cc-pVTZ basis set with additional five tight *s* functions is used in HFC calculations, as this basis is flexible in core and valence regions and gives a balanced description of electron correlation and electron density near the nucleus [37]. The nuclear spin–rotation coupling constant is calculated using rotational orbitals which give an improved basis set convergence [36].

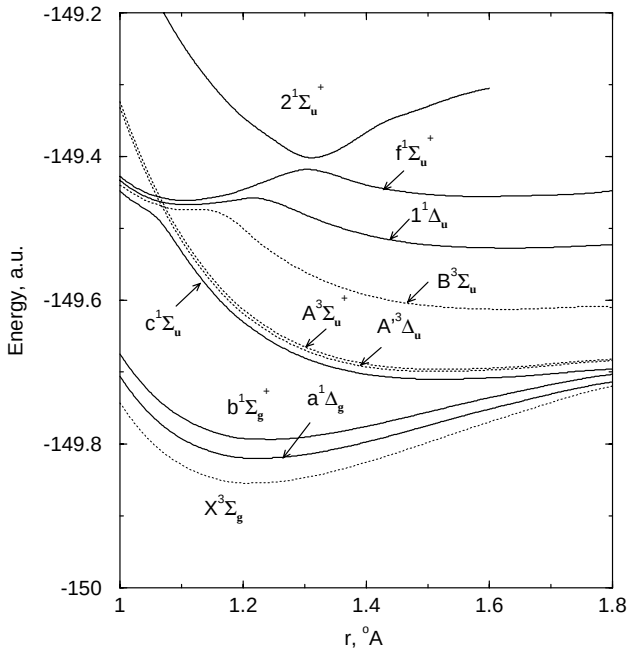

Fig. 1. Potential energy curves of the $\pi\pi^*$ states of O_2 molecule. Three lowest states calculated by MCSCF 10-CAS method (3–4σ_g, 2–3σ_u, 1–2π_u, 1–2π_g) with the aug-cc-pVTZ basis set. The upper singlet states are obtained by linear response calculations with the $b^1\Sigma_g^+$ state as a reference. The $\sigma\pi$ ($^{1,3}\Pi_u$, g) states are not shown for simplicity.

The MCSCF calculations were performed with the DALTON [38] program packages. The spin density at the nuclei is calculated also by the unrestricted Hartree–Fock (UHF) method [25] with GAMESS code [39]. Linear response technique is implemented in DALTON for excited states energy and properties calculations with analytic first- and second-derivative techniques [28,36,38]. Since many of the studied properties depend on excited states energy, electric and magnetic dipole transition moments, the potential energy curves for a number of important excited states are also presented (Fig. 1). They have been calculated by the 10-CAS-T method (aug-cc-pVTZ basis is denoted by "T" letter) as in [40]. In comparison with Fig. 1 from [40] the potential curve of the $B^3\Sigma_u^-$ state is improved at small internuclear distances by account of larger number of roots in response procedure.

3. Results and discussion

The ground state of O_2 molecule is the triplet state with zero orbital angular momentum, and hence is a good Hund's case (*b*) [15]. The coupling between electron spin *S* and rotation *K* is about 60 GHz [2,21], whereas the hyperfine coupling between *S* and nuclear spin *I* for ^{17}O in $^{16}O^{17}O$ isotope species is only a few hundred MHz, so the $^{16}O^{17}O$ isotope species represents a rather good case ($b_{\beta J}$) [15]. The coupling of *I* to *K* which depends on the electric quadrupole interaction is only about 3 MHz [41]; the direct *I* to *K* interaction is much weaker (about 55 kHz [13]), thus the *J* representation ($b_{\beta J}$) is the best.

The observed hyperfine structure in the microwave spectrum of the $^{16}O^{17}O$ molecule can be interpreted with the following zero-field spin-Hamiltonian [13,14,41]:

$$H = b(I,S) + cI_zS_z + f(K,I) + \frac{e^2Q_Oq_{zz}}{4I(2I-1)}(3I_z^2 - I^2). \quad (2)$$

The first two terms represent the hyperfine interaction between the nuclear and electron spins, the third term represents the nuclear spin–rotation coupling and the last one describes the nuclear quadrupole coupling. The constants *b* and *c* are determined by the unpaired spin density [41]:

$$b = 2g_I\mu_0\mu_N\left[\frac{8\pi}{3}\psi^2(0) - \left(\frac{3\cos^2\theta - 1}{2r^3}\right)_{av}\right], \quad (3)$$

$$c = 6g_I\mu_0\mu_N\left(\frac{3\cos^2\theta - 1}{2r^3}\right)_{av}, \quad (4)$$

where av means averaging, g_I is the g factor for ^{17}O ($g_I = -0.76$) [13], μ_N the nuclear magneton, μ_0 the Bohr magneton, both are assumed to be positive in sign, θ the angle between the molecular axis and the vector $\boldsymbol{r}$ joining the nucleus with the electron, $\psi^2(0)$ is the density of unpaired electron spins at the ^{17}O nucleus. The measured values of the HFC constants are: $b = -101.4$ MHz and $c = 140$ MHz [13,41]. From these constants, a direct determination of two important properties of the ground state wave function follows:

$$\psi^2(0) = 1.26\,\text{Å}^{-3} = 0.1867a_0^{-3}, \quad (5)$$

$$\left\langle\frac{P_2}{r^3}\right\rangle = \left(\frac{3\cos^2\theta - 1}{2r^3}\right)_{av} = -8.9\,\text{Å}^{-3} = -1.3188a_0^{-3}, \quad (6)$$

where a_0 means the Bohr radius. The negative value of $\langle P_2/r^3\rangle$ shows that the unpaired electrons are primarily in the π_g-MO, as follows from the main configuration (Eq. (1)); even simple calculations reproduce the observed value, Eq. (6) [14]. Explanation of the result given by Eq. (5) is not so simple. For the pure ground state configuration wave function (Eq. (1)) only p_π orbitals contribute to the spin density, thus $\psi^2(0) = 0$ in a great contradiction with the observed HFC constants of the microwave spectrum of $^{16}O^{17}O$ [14]. A small admixture of the excited configurations:

$$^3\psi_1[^3\Sigma_g^-] = \mathcal{A}(1\sigma_g)^2(1\sigma_u)^2(2\sigma_g)^2(2\sigma_u)^2 \times (3\sigma_g)^1(\pi_u)^3(\pi_g)^3(3\sigma_u)^1, \quad (7)$$

provides appreciable contribution to the $\psi^2(0)$ value. Four determinants which constitute this $^3\psi_1[^3\Sigma_g^-]$ configuration wave function have slightly non-equal coefficients:

$$\begin{aligned}&0.056[|(3\sigma_g\alpha)(\pi_{u,x}\alpha)(\pi_{u,y})^2(\pi_{g,x})^2(\pi_{g,y}\alpha)(3\sigma_u\beta)|\\&\quad -|(3\sigma_g\alpha)(\pi_{u,x})^2(\pi_{u,y}\alpha)(\pi_{g,x}\alpha)(\pi_{g,y})^2(3\sigma_u\beta)|]\\&\quad -0.070[|(3\sigma_g\alpha)(\pi_{u,x}\beta)(\pi_{u,y})^2(\pi_{g,x})^2(\pi_{g,y}\alpha)(3\sigma_u\alpha)|\\&\quad -|(3\sigma_g\alpha)(\pi_{u,x})^2(\pi_{u,y}\beta)(\pi_{g,x}\alpha)(\pi_{g,y})^2(3\sigma_u\alpha)|].\end{aligned}$$

Thus, the α spin density prevails on the $(3\sigma_u)$-MO, which is characterised by appreciable contribution from s-functions with large density at the nuclei. Large contribution to the spin density comes also from the crossed terms $^3\psi_1 - {}^3\psi_0$ [18]. The value $\psi^2(0)$ calculated at the 10-CAS-T level (Table 1) is not in a good agreement the observed HFC structure [14].

The aug-cc-pVTZ basis set with polarization wavefunctions does not describe proper behaviour at the nuclei. Much better results are obtained with the uncontracted aug-cc-pVTZ basis set with additional five tight s functions [37]. At the equilibrium distance $r_e = 1.207536$ Å we get $\psi^2(0) = 0.1893a_0^{-3}$ in a good agreement with the value extracted from the observed microwave spectrum [14].

Table 2
The ground state $X^3\Sigma_g^-$ properties of the O_2 molecule calculated by UHF method with different basis sets at $r = 1.217$ Å

Basis	E (a.u.)	$\psi^2(0)$, a_0^{-3}	Q_{zz}, ea_0^2
3-21G	−148.768370	0.324	−0.808
6-31G	−149.545014	0.437	−0.886
6-311G	−149.595716	0.355	−0.844
6-311++G(d, p)	−149.662585	0.346	−0.231
TZV	−149.610054	0.342	−0.744
STO-3G	−147.634171	0.133	−1.020
STO-5G	−148.968781	0.188	−0.879
STO-6G	−149.052202	0.208	−0.879
Experiment	–	0.187[a]	−0.25[b]

[a] From [14,18].
[b] From [10,19].

It is interesting to note that Slater-type orbitals (STO) give good HFS constants at simple level of theory [18]. Kotani at el. have reproduced the observed $\psi^2(0)$ value by simple CI calculation with the STO basis at the fixed distance ($r = 2.3a_0 = 1.217$ Å); they have got $\psi^2(0) = 0.195a_0^{-3}$ with the 15 configurational wave function [18]. The simplest way to calculate the HFC constants provides the unrestricted UHF method [42]. The $\psi^2(0)$ values calculated by the UHF method with different basis sets at the same ($r = 2.3a_0$) distance are presented in Table 2. The ground state energy and quadrupole moment are also given. Though the STO-5G method gives rather poor total energy the calculated $\psi^2(0)$ value is in an excellent agreement with the experimental HFC parameter [14]. The internuclear distance dependence of the $\psi^2(0)$ value calculated by the UHF method with the STO-5G basis is presented in Fig. 2. This is a descending function of r and all methods reproduce this trend. The splitted basis sets of the 6-31G type strongly overestimate the HFS constant; extension of polarization functions does not improve the $\psi^2(0)$ value, but improves the calculated quadrupole moment. This property is discussed in more details in Section 3.1.

3.1. Quadrupole moment of O_2 molecule

As one can see from Table 2, only the basis set with large number of polarization functions (6-311++G(d, p)) gives the correct quadrupole moment in UHF method. In MCSCF method, the quadrupole moment value strongly depends on the active space. Results of the electric quadrupole moment calculations by MCSCF method with different CAS at the experimentally determined equilibrium bond length are presented in Table 1. The distance dependence of the quadrupole moment is shown in Fig. 3. The quadrupole moment strongly depends on the proper balance of the empty $2\pi_g4\sigma_g$ and $2\pi_u4\sigma_u$ MOs account in the CAS. Even a small active space, 1-CAS (Table 1), where g–u orbitals are equally accounted, provides a reasonable Q_{zz} value, while the larger CASs (i = 3–5, 7–10) predict an underestimation of the $|Q_{zz}|$ component. The quadrupole tensor is traceless

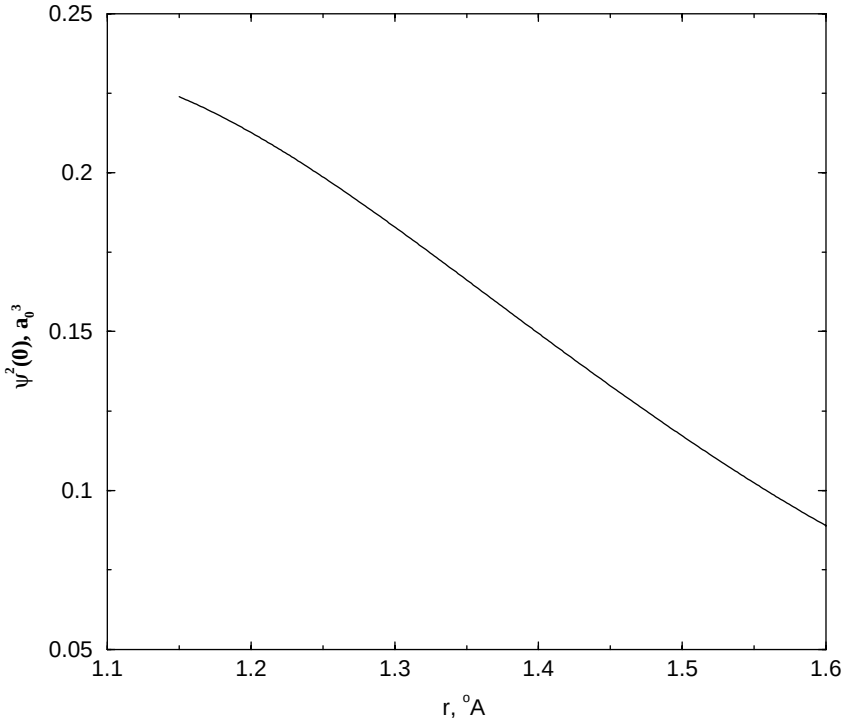

Fig. 2. Spin density at the nuclei calculated by UHF method (STO-5G basis set) for the ground $X^3\Sigma_g^-$ state of O_2 molecule as a function of the internuclear distance r (Å).

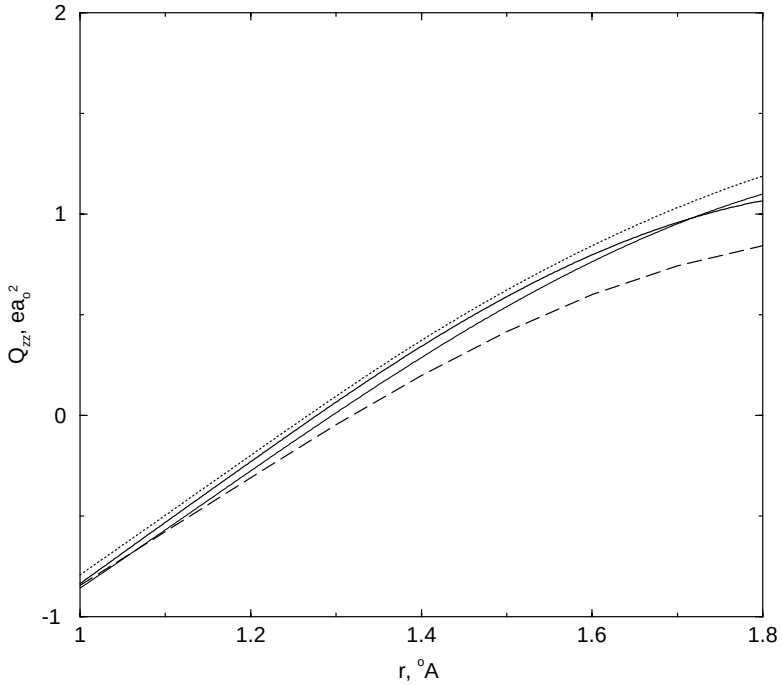

Fig. 3. The parallel component (Q_{zz}) of the quadrupole moment tensor (a.u.) calculated by MCSCF method with different CAS for the ground $X^3\Sigma_g^-$ state of O_2 molecule as a function of the internuclear distance r (Å): long dashed line (1-CAS-T); solid line (6-CAS-T); dotted line (10-CAS-T); bold solid line (11-CAS-T) (1 a.u. $= e \times \text{Bohr}^2 = 1.3441$ Buckingham (10^{-26} esu cm^2)).

($Q_{xx} = Q_{yy} = -(1/2)Q_{zz}$). Comparison indicates that small CAS calculation overestimates the $|Q_{zz}|$ quadrupole tensor component near r_e point and predicts not such a strong r-dependence like the larger CASs do (Fig. 3).

The scalar $q = Q_{zz}/e$ is often referred to the quadrupole moment of diatomic. There are few measurements of q in the ground state O_2 molecule. The old results are: $q = -0.11 \times 10^{-16}\,\mathrm{cm}^2$ obtained from collision diameter and $q = -0.04 \times 10^{-16}\,\mathrm{cm}^2$ obtained from the line widths of the microwave spectrum of oxygen [43]; these values correspond to Q_{zz} equal to $-0.393ea_0^2$ and $-0.143ea_0^2$, respectively (here e is positive). Buckingham et al. [44] have obtained the O_2 quadrupole moment from induced birefringence $Q_{zz} = -0.4 \times 10^{-26}\,\mathrm{esu\,cm}^2 = -0.298ea_0^2$. The most accurate quadrupole moment has been extracted from the pressure-induced far-infrared spectrum analysis: $Q_{zz} = -0.35 \times 10^{-26}\,\mathrm{esu\ cm}^2 = -0.26ea_0^2$ [10]. The largest and well-balanced active space, 11-CAS, reproduces the last value pretty well (Table 1). The basis set and CI active space dependence of the O_2 quadrupole moment have been discussed by Rijks at el. [19]: they have presented Q_{zz} values from -0.31 till $-0.27ea_0^2$ by subsequent improve of the total energy. Rijks at el. have found that the final increase of the basis set, which lowers the total energy only slightly, produces considerable improvement of the quadrupole moment [19]. From Fig. 3, it follows that the Q_{zz} value changes sign at $r \sim 1.27$–1.32 Å, thus it is close to zero near the equilibrium; small deviations in the slope of the function $Q_{zz}(r)$ lead to large differences in the calculated quadrupole moment of the ground state oxygen.

3.2. Nuclear quadrupole coupling constant of $^{17}O_2$ and $^{17}O^{16}O$ molecules

The NQC constant, $e^2Q_Oq_{zz}$, is a measure of the electric nuclear quadrupole moment (Q_O) interaction with the gradient of the electric field at the site of the nucleus [13]. The NQC constant for the ground state oxygen molecule can be calculated for the ^{17}O isotope; the nuclear quadrupole moment is $eQ_O = -0.02558 \times 10^{-24}e\,\mathrm{cm}^2$, spin is $I = 2.5$ [36]. If one neglect very weak vibronic effects and the small difference in the r_e values, the NQC constant is the same for $^{17}O_2$ and $^{17}O^{16}O$ molecules. The NQC constant in diatomic is a tensor of the type: $V_{xx} = V_{yy} = -(1/2)V_{zz}$, where $V_{zz} = e^2q_{zz}Q_O/h$. The V_{zz} value (in MHz) calculated by 10-CAS-T method is presented in Fig. 4; the same values calculated by different CAS are given in the Table 1. Experimental NQC constant was measured in the ESR spectrum of gaseous $^{16}O^{17}O$ for the ground state: $V_{zz} = -8.42 \pm 0.18$ MHz [13]. All active spaces produce a reasonable qualitative agreement at the experimental equilibrium O–O distance $r_e^{exp} = 1.2075$ Å (Table 1.) The NQC constant does not depend much on the CAS (Table 1). The basis set convergence in the aug-cc-pVNZ group is pretty fast; even in 1-CAS-D we get a reasonable value $V_{zz} = -7.74$ MHz. The more important is the internuclear distance dependence of the NQC constant (Fig. 4). The absolute $|V_{zz}|$

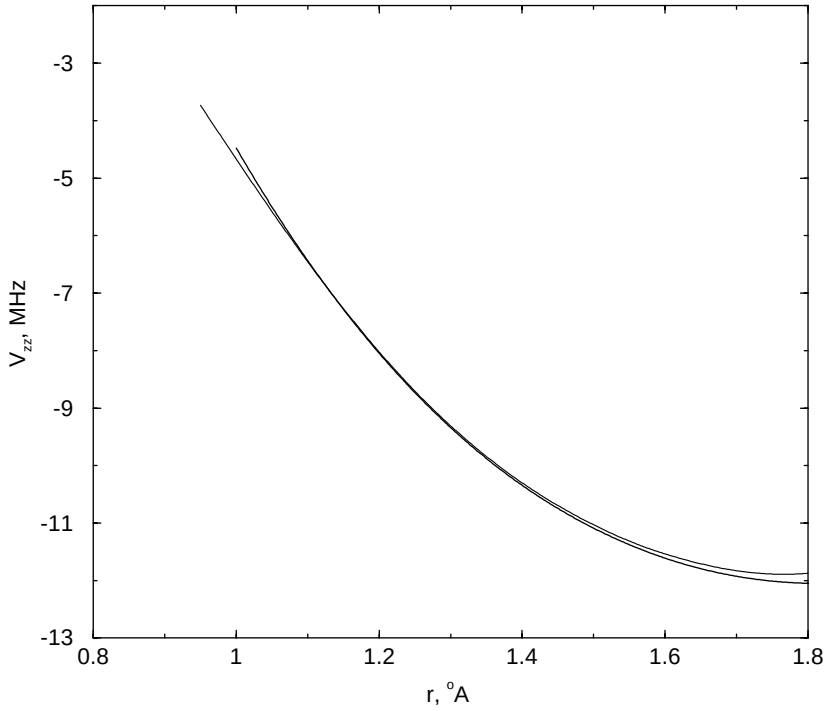

Fig. 4. The nuclear quadrupole coupling constant V_{zz} (MHz) calculated by MCSCF methods for the ground $X^3\Sigma_g^-$ state of O_2 molecule as a function of the internuclear distance r (Å): thin line (10-CAS-T); bold line (11-CAS-T) (1 a.u. = −6.010395 MHz).

value increases with the internuclear distance; thus, vibrational averaged NQC constant $|V_{zz}|$ values is slightly larger than $|V_{zz}|$ at r_e distance. At the calculated equilibrium distance in the 11-CAS-T method ($r_e^{cal} = 1.214$ Å) the NQC constant is $V_{zz} = -8.252$ MHz and the vibrational averaged value equals −8.31 MHz in a good agreement with the ESR spectrum measurement [13].

3.3. Polarizability

Static and dynamic polarizability of the ground state oxygen molecule have been studied in a number of works (for a recent review, see [9,19,20,32,45]). Previous MCSCF calculations with the aug-cc-pVDZ basis and 9-CAS [32] have given $\alpha_{xx} = 7.32a_0^3$ and $\alpha_{zz} = 14.55a_0^3$, which are close to the present MCSCF calculations with the aug-cc-pVTZ basis (Table 1). An extension of the active space to the 10-CAS deteriorates the α_{xx} value ($6.51a_0^3$). Account of all valence 12 electrons in the active space provides a good agreement with experiment (Table 1) for the perpendicular component of the polarizability tensor. The largest and well-balanced 11-CAS again provides (like in the quadrupole tensor calculations) a very good agreement with experiment for the whole polarizability tensor (Table 1): the calculated anisotropy is $7.41a_0^3$, while the frequency corrected experimental value is $7.29a_0^3$ [9]. The calculated mean value of the static polarizability is $10.51a_0^3$ (experiment gives $10.59a_0^3$ [9]). The α_{zz} component strongly increases with internuclear distance r; in the range 1.1–1.5 Å. It is almost linear function of r with the slope determined by the angle ϕ: tg $\phi = 10.8$ (Fig. 5) The perpendicular component of the polarizability ($\alpha_{xx} = \alpha_{yy}$) is not such a strong function of r. A large contribution to α_{zz} component is produced by electric dipole transition moment to the $B^3\Sigma_u^-$ state, which is pretty high until $r < 1.6$ Å [32,33,45]. The transition energy, which comes to the denominator of the α_{zz} polarizability expression, strongly decreases with r (Fig. 1); this explains the α_{zz} behavior (Fig. 5). At the same time transitions to the $^3\Pi_u$ states have small intensity [33,45]. Thus, the perpendicular α_{xx} component only slightly increases with r, though the transitions energy also decrease with bond distance [32,45].

3.4. Magnetic susceptibility

The dominant contribution to the interaction of O_2 molecule with magnetic field (H) is that between the electronic spin magnetic moment (S) and the external field: $H_{Zeeman} = -\mu_0 HgS$ [12]. The electronic g factor has been calculated before by MCSCF method to be $g_{xx} = g_{yy} = 2.0050$ [29] in a reasonable agreement with experimental value 2.0048 [46]. The shift of the calculated g factor from the free electron value ($2.0023 \simeq g_{zz}$) depends on the spin–orbit coupling (SOC) mixing between the ground $X^3\Sigma_g^-$ state and the triplet $^3\Pi_g$ states and strongly increases with the internuclear distance [2,29]. The zero-field magnetic moment of O_2 molecule includes also (behind spin) the rotational moment K contribution [12,15]:

$$\mu = \mu_0(gS + g_r K), \quad (8)$$

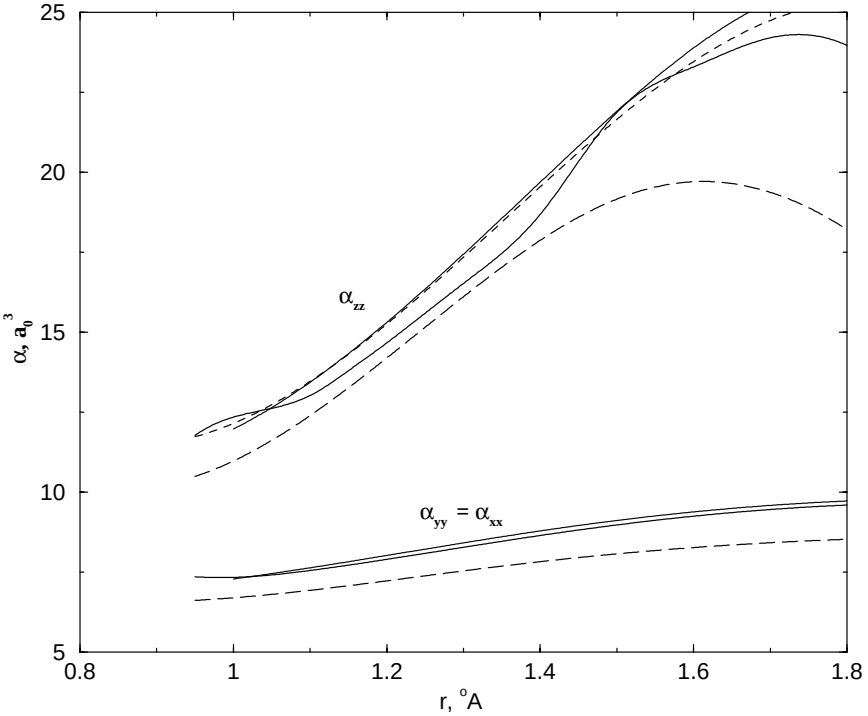

Fig. 5. Static polarizability of the ground $X^3\Sigma_g^-$ state of O_2 molecule as a function of the internuclear distance r (Å): long dashed line (1-CAS-T); solid line (6-CAS-T); dashed line (10-CAS-T); bold solid line (11-CAS-T) (1 a.u. = 0.14818471 Å^3).

where g_r is rotational g factor. An applied magnetic field induces a new magnetic moment to an extent determined by magnetic susceptibility χ. Interaction of molecular oxygen with a magnetic field has been completely treated by Tinkham and Strandberg [12]. The molar susceptibility of the dioxygen includes the temperature dependent spin part, $N_0 g^2 \mu_0^2 S(S+1)/3kT$, and the temperature-independent terms:

$$\chi = \frac{4N_0}{3}\mu_0^2 \sum_n \frac{|\langle 0|L_x|n\rangle|^2}{E_n - E_0} - \frac{N_0 e^2}{6mc^2}\sum_i \langle 0|r_i^2|0\rangle, \qquad (9)$$

where N_0 is the Avogadro number and L_x is the operator of the orbital angular momentum projection on x-axis (perpendicular to O–O axis) [12,47]. Sometimes [11] the temperature-independent term, Eq. (9), is called diamagnetic susceptibility in contrast to the temperature dependent spin part. This leads to a confusion, since the second term in Eq. (9) is also called a diamagnetic contribution (χ^{dia}), and the first one is called a paramagnetic (or high-frequency) contribution (χ^{para}) [12,47].

Both contributions have opposite signs and nearly cancel each other: they were estimated as $\chi^{para} = 24.6 \pm 1.7 \times 10^{-6}\,cm^3\,mol^{-1}$ and $\chi^{dia} = -29.5 \times 10^{-6}\,cm^3\,mol^{-1}$ [12]. Thus, the temperature-independent part of the isotropic magnetic susceptibility, Eq. (9), estimated by Tinkham and Strandberg [12] is equal to $-4.9 \pm 1.7 \times 10^{-6}\,cm^3\,mol^{-1}$. Kotani at el. [18] have obtained $\chi^{dia} = -31.3 \times 10^{-6}\,cm^3\,mol^{-1}$ with their 15 configurational wave function; together with χ^{para}, estimated by Tinkham and Strandberg from rotational g_r factor, it yields the temperature-independent part of the susceptibility of $-7.3 \times 10^{-6}\,cm^3\,mol^{-1}$ [18].

The temperature-independent part of the magnetizability tensor at zero field can be calculated directly as energy derivative. For diatomic molecule the perpendicular component, for example, is equal to [36]:

$$\chi_{xx} = -\mu_0 \frac{d^2 W}{dH_x^2}, \qquad (10)$$

where H is the external magnetic field. The electronic energy $W(H)$ is obtained by optimizing the electronic energy function with respect to variational parameters [38,48]. Direct MCSCF calculations of the magnetizability tensor made in the present work indicate that both the paramagnetic and diamagnetic parts of the perpendicular $\chi_{xx} = \chi_{yy}$ components are strong function of the internuclear distance; they do compensate each other completely at the point $r = 1.42$ Å, where $\chi_{xx} = \chi_{yy}$ comes to zero (Fig. 6). At shorter distances the negative diamagnetic part prevails, at longer r the paramagnetic contribution is higher. The parallel component χ_{zz} has no paramagnetic contribution and it is not a strong function of the internuclear distance (Fig. 6). One can see that the parallel component is almost constant ($\chi_{zz} \sim -3.8$ a.u.), but the perpendicular components are strong functions of r. The perpendicular components have large negative diamagnetic contribution ($\chi_{xx}^{dia} \sim -9$ a.u.) and large positive paramagnetic contribution ($\chi_{xx}^{para} \sim 8$ a.u.); these values correspond to the vicinity of r_e distance (Fig. 7). Absolute values of the both contributions increase with r but paramagnetic part increases faster, so the χ_{xx}

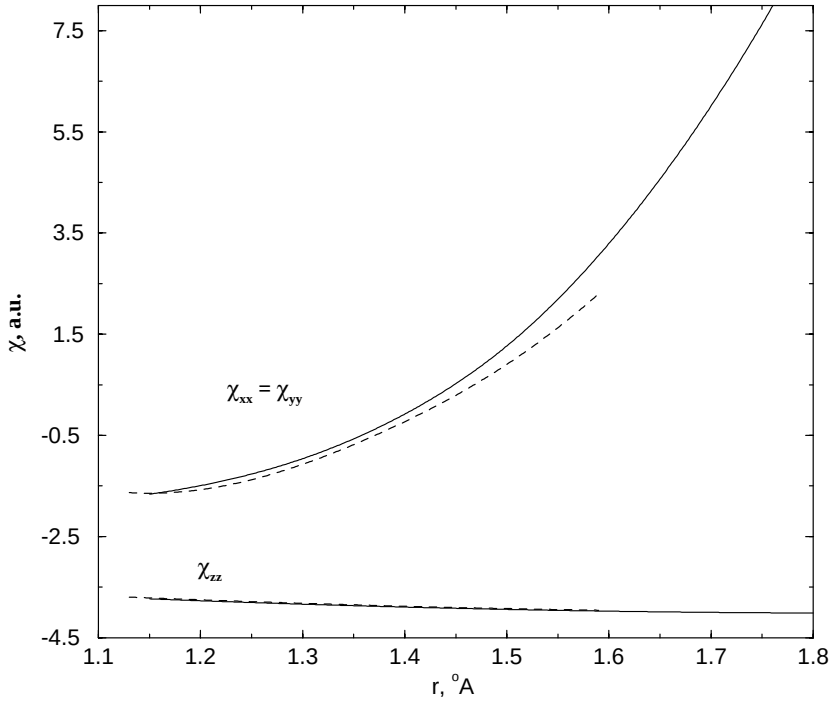

Fig. 6. Magnetizability tensor calculated by MCSCF method (10-CAS-T) for the ground $X^3\Sigma_g^-$ state of O_2 molecule as a function of the internuclear distance r (Å): thin line (10-CAS-T); bold line (11-CAS-T) (1 a.u. = $4.75181661 \times 10^{-6}\,cm^3\,mol^{-1}$).

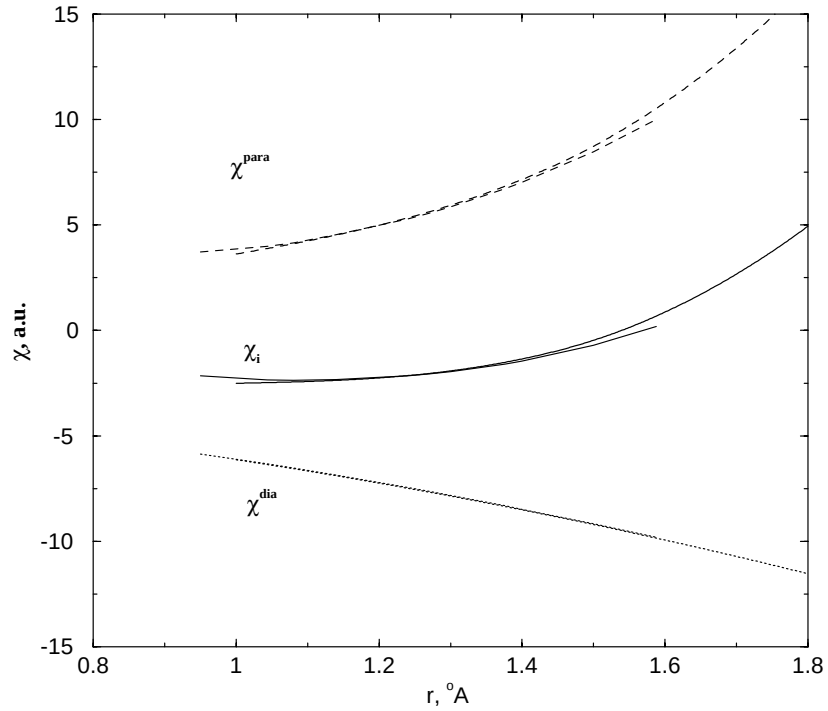

Fig. 7. Isotropic magnetizability and its diamagnetic and paramagnetic contributions calculated by MCSCF method for the ground $X^3\Sigma_g^-$ state of O_2 molecule as a function of the internuclear distance r (Å): thin line (11-CAS-T); bold line (10-CAS-T).

perpendicular component rises with the distance and is getting positive at $r \geq 1.42$ Å (Fig. 6). Similar trends have been obtained for the $b^1\Sigma_g^+$ and $c^1\Sigma_u^-$ states [40]. The isotropic magnetizability (χ_i) at the optimized equilibrium distance $r_e = 1.2347$ Å in the b state calculated by the 11-CAS-T method is $\chi_i = -1.94$ a.u. $= -9.20 \times 10^{-6}$ cm^3 mol^{-1}; thus, it is predicted to be slightly different from the isotropic (temperature-independent) magnetizability of the ground state.

In Table 1 and Fig. 6, the χ_{aa} tensor components are given in atomic units: 1 a.u. $= 4.75182 \times 10^{-6}$ cm^3 mol^{-1}. The isotropic susceptibility $\chi_i = (1/3)(\chi_{zz} + 2\chi_{xx})$ obtained with the 11-CAS-T method (Fig. 7) is -2.235 a.u. $= -10.62 \times 10^{-6}$ cm^3 mol^{-1}. Thus, the calculated $|\chi_i|$ value is larger than the previous estimations of Kotani at el. [18] and Tinkham and Strandberg [12]. The calculated paramagnetic component of the isotropic susceptibility (Fig. 7), $\chi^{para} = 24.02 \times 10^{-6}$ cm^3 mol^{-1}, is in excellent agreement with the result of Tinkham and Strandberg obtained from the measured g_r factor [12]; the diamagnetic part obtained in the present work (Fig. 7) is $\chi^{dia} = -34.64 \times 10^{-6}$ cm^3 mol^{-1}; it deviates more from previous calculations [12,18]. These values are calculated at the experimental r_e distance. In the vicinity of the optimized equilibrium (1.214 Å in 11-CAS) the magnetic susceptibility tensor does not change fast with r; the isotropic susceptibility slightly changes to -10.54×10^{-6} cm^3 mol^{-1} (χ^{para} and χ^{dia} are equal to 24.30 and -34.84×10^{-6} cm^3 mol^{-1}, respectively).

Anisotropy of the temperature-independent part of the magnetic susceptibility of molecular oxygen has been derived from the magnetic field induced birefringence (Cotton–Mouton effect) [11]: $\chi_{zz} - \chi_{xx} = -17.7 \times 10^{-30}$ cm^3, which corresponds to the molar anisotropy of magnetizability equal to -10.66×10^{-6} cm^3 mol^{-1}. This is in excellent agreement with the 11-CAS result: $\chi_{zz} - \chi_{xx} = -2.312$ a.u. $= -10.98 \times 10^{-6}$ cm^3 mol^{-1}.

The temperature-dependent part of the molar magnetic susceptibility of molecular oxygen calculated with account of the electronic g factor in the same 11-CAS-T method ($g_{xx} = 2.0052$) is equal to $1.003/T$ cm^3 mol^{-1}. At $T = 293$ K this temperature-dependent spin part of susceptibility is equal to 3.42×10^{-3} cm^3 mol^{-1}, which is much higher than the temperature-independent part, calculated with the same 11-CAS-T method (-10.6×10^{-6} cm^3 mol^{-1}). The last correction is still too small compared to the spread in the measured values (3.48–3.33) $\times 10^{-3}$ cm^3 mol^{-1} [47]; it cannot explain small deviations from the Curie's law, which might be ascribed to measurement error [47]. The most accurate and usually accepted molar susceptibility of molecular oxygen at 293 K is 3.45×10^{-3} cm^3 mol^{-1} [47,49], which is in a good agreement with our value. It is difficult to measure the temperature-independent (or diamagnetic [11]) susceptibility of paramagnetic molecular oxygen. Rotational Zeeman effect provides a complementary tool for this estimation since the electronic part of rotational g_r factor is connected with χ^{para} (Eq. (9)) [12,15,47].

Table 3
Molecular g factor of the $X^3\Sigma_g^-$ state and nuclear spin–rotation constants, M_O in kHz (including nuclear part, diamagnetic and paramagnetic contributions) of all possible isotope modifications of O_2 molecule calculated at $r = 1.207536$ Å by MCSCF method with the "aug-cc-pVTZ" basis sets and small complete active space (1-CAS)

Isotope	Spin–rotation constant (kHz)				Molecular g factor			
	$M_{O,tot}$	Nuclear	Diamagnetic	Paramagnetic	Isotropic	Nuclear	Diamagnetic	Electronic
^{16}O–^{16}O	–	–	–	–	−0.2075	0.5038	−0.0640	−0.6473
^{16}O–^{17}O	22.0136	−3.2393	1.3157	23.9371	−0.2014	0.4894	−0.0621	−0.6286
^{16}O–^{18}O	–	–	–	–	−0.1960	0.4774	−0.0606	−0.6127
^{17}O–^{17}O	21.3440	−3.1407	1.3062	23.1783	−0.1953	0.4740	−0.0602	−0.6090
^{17}O–^{18}O	20.7508	−3.0534	1.2977	22.5066	−0.1898	0.4612	−0.0586	−0.5925

Moment of inertia (in amu Å^2, where amu is atomic mass units) at r_e distance (1.207536 Å) is 41.643752 for the ^{16}O–^{16}O isotope, 44.258291 for the ^{17}O–^{17}O isotope, 45.522911 for the ^{17}O–^{18}O isotope, 42.91122 for the ^{16}O–^{17}O isotope, and 44.0990 for the ^{16}O–^{18}O isotope.

3.5. Rotational Zeeman effect and rotational g_r factor

The coupling of molecular rotation with electronic motion gives rise to a weak magnetic interaction that plays an important role in analysis of rotational spectra by the Zeeman effect [15]. Rotational g_r factor describes the dependence of rotational energy levels on the external magnetic field, H, and arises from the interaction of the rotationally induced molecular magnetic moment with the field H. The rotational g_r factor is proportional to the ratio of the magnetic moment to the molecular rotational angular momentum; this quantity indicates the extent of the splitting of rotational energies. The corresponding energy correction to the rotational energy levels is [36]:

$$\Delta E = -\mu_N H g_r K, \tag{11}$$

where K is the total rotational angular momentum, μ_N the nuclear magneton. Rotational g_r tensor have been calculated here by MCSCF method as second derivative of the total energy with respect to H and K (Tables 3–5, Fig. 8). In order to compute this derivative it is necessary to include the coupling of rotational and electronic motions in the electronic

Table 4
Nuclear spin–rotation coupling constant, M_O in kHz, and isotropic molecular g_r factor of the $X^3\Sigma_g^-$ state (including diamagnetic and paramagnetic contributions) of ^{16}O–^{17}O isotope modification calculated by MCSCF method with the "aug-cc-pVTZ" basis sets and 10-CAS

r (Å)	Spin–rotation constant (kHz)				Molecular g factor		
	$M_{O,tot}$	Nuclear	Diamagnetic	Paramagnetic	Isotropic	Diamagnetic	Electronic
1.000	18.9720	−5.7036	2.4607	22.2150	−0.2608	−0.0571	−0.6931
1.2075	22.0136	−3.2393	1.3157	23.9371	−0.2014	−0.0621	−0.6286
1.300	24.1610	−2.5961	1.0463	25.7108	−0.2089	−0.0631	−0.6352
1.400	26.7607	−2.0786	0.8428	27.9964	−0.2276	−0.0637	−0.6532
1.500	29.5003	−1.6900	0.6999	30.4904	−0.2527	−0.0641	−0.6779
1.600	32.1596	−1.3925	0.5970	32.9551	−0.2804	−0.0643	−0.7055
1.700	34.3776	−1.1609	0.5209	35.0177	−0.3065	−0.0644	−0.7315
1.800	35.8079	−0.9780	0.4629	36.3230	−0.3275	−0.0644	−0.7524

The nuclear part contribution to the NSRC constant is also presented. Nuclear part of g_r factor is equal to 0.48937. Nuclear g value of the ^{17}O isotope is equal to −0.76.

Table 5
Molecular g factor of the $X^3\Sigma_g^-$ state and nuclear spin–rotation constants, MO in kHz (including nuclear part, diamagnetic and paramagnetic contributions) of all possible isotope modifications of O_2 molecule calculated at $r = 1.22$ Åby MCSCF method with the "aug-cc-pVDZ" basis sets and small complete active space $\pi_u\pi_g$ ($6e \times 4$ MOs)

Isotope	Spin–rotation constant (kHz)				Molecular g factor				
	$M_{O,tot}$	Nuclear	Diamagnetic	Paramagnetic	Isotropic	Nuclear	Diamagnetic	Electronic	Experiment[a]
^{16}O–^{16}O	–	–	–	–	−0.2386	0.5038	−0.1213	−0.6211	−0.2355
^{16}O–^{17}O	24.6303	−3.1410	0.9397	26.8316	−0.2315	0.4894	−0.1178	−0.6031	−0.2300
^{16}O–^{18}O	–	–	–	–	−0.2253	0.4774	−0.1149	−0.5878	–
^{17}O–^{17}O	23.8823	−3.0454	0.9163	26.0115	−0.2245	0.4740	−0.1141	−0.5844	–
^{17}O–^{18}O	23.2190	−2.9608	0.8955	25.2843	−0.2183	0.4612	−0.1110	−0.5685	−0.2226
^{18}O–^{18}O	–	–	–	–	−0.2120	0.4477	−0.1078	−0.5520	−0.2171

[a] Values from [13] are multiplied by $m/M = 1840$.

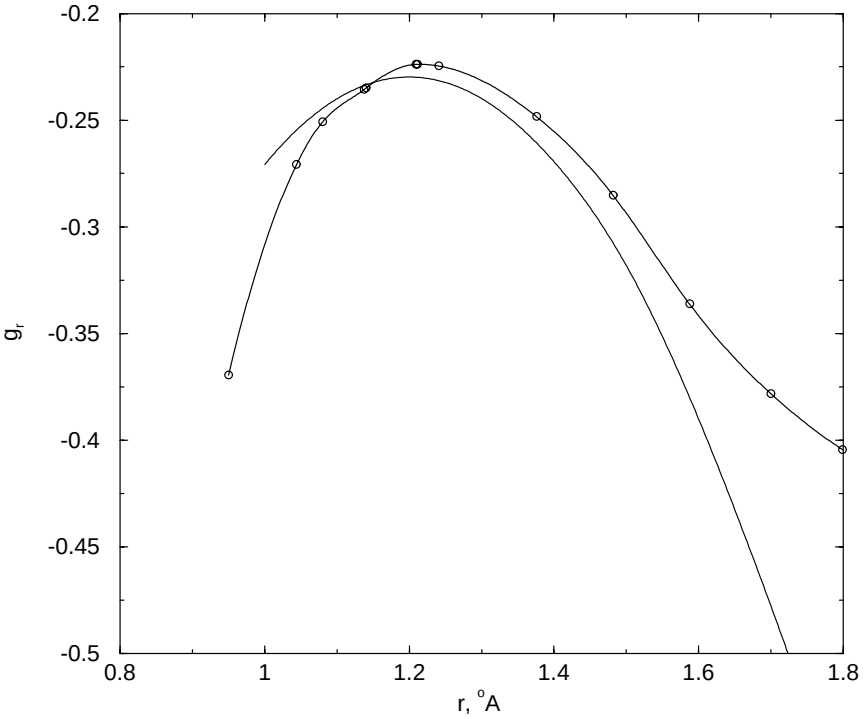

Fig. 8. Rotational g_r factor calculated by MCSCF method for the ground $X^3\Sigma_g^-$ state of O_2 molecule as a function of the internuclear distance r (Å): thin line (10-CAS-T); bold line (11-CAS-T).

Hamiltonian and the internal field due to the nuclear magnetic moment (for isotope ^{17}O) [36,38]. In Table 3, the molecular g_r factor for the ground state oxygen with different isotope modification are presented; g_r factor has been calculated at $r_e = 1.207536$ Å distance with 1-CAS-T method. Similar results are obtained with 6-CAS-D and 10-CAS-D methods. Comparison indicates the same trends in the g_r factor shifts for different isotopes. For example, transition from $^{16}O_2$ to $^{16}O^{17}O$ produces the g_r factor shift about 0.006. The molecular g_r factor consists of two terms: a nuclear part which is determined by nuclear masses (for $^{16}O_2$ molecule it is $Z/A = 8/15.9949 = 0.5038$ in m/M units) and electronic part which is actually connected with a paramagnetic contribution to the magnetizability evaluated with the gauge origin being the centre of mass [12,36]:

$$g_r^e = -4Re \sum_n \frac{\langle 0|L_x|n\rangle\langle n|BL_x|0\rangle}{E_n - E_0}, \quad (12)$$

where $B = h/8\pi^2 c\mu r^2$ is a rotational constant operator, μ is a reduced mass. Only perpendicular component of the g_r tensor has non-zero value. The sums in Eqs. (9) and (12) are very similar, if B is a constant and does not induce any difference in the variational treatment by Eqs. (10) and (11). Our results for different isotopes with different CAS and r values indicate that the electronic parts of g_r factor can be treated by putting B out of the integral in Eq. (12). The g_r factors presented in this work are expressed in m/M units, where m and M are masses of electron and proton, respectively. Rotational g_r factors presented in experimental works [12,13,46] are $(M/m) = 1840$ times smaller.

Calculations indicate that g_r factor is a strong function of internuclear distance. The nuclear contribution to the g_r factor does not depend on r, but only on the mass of the isotope. Electronic parts of g_r factor are different for various isotope modifications, which is quite natural. Since B constant decreases fast with increase of the distance r, one can anticipate that $|g_r^e|$ (and hence $|g_r|$) value should decrease. The calculated g_r distance dependence (Fig. 8) does not support this simple consideration. In Fig. 8 the g_r values for oxygen $^{16}O_2$ calculated by the MCSCF method in the 10-CAS-T and 11-CAS-T approaches are presented at different internuclear distances. There is a clear maximum just at the equilibrium r_e distance; to the left from the maximum we get the generally anticipated $|g_r|$ dependence on r. But to the right from the maximum the $|g_r|$ value increases because the electronic part $|g_r^e|$ strongly depends on the magnetic dipole transition moments $\langle X^3\Sigma_g^-|L_x|^3\Pi_g\rangle$. The energy gap in denominator of Eq. (12) decreases with r at large distances, but the magnetic dipole transition moments do not change much [2,24,34]; thus, the $|g_r^e|$ value rises. By the same reasons the values of the electronic g factor [29], of the orbital contribution to the $b^1\Sigma_g^+ - X^3\Sigma_g^-$ transition moment $(-L_{b-X})$ [2,34] and of the perpendicular component of magnetizability increase with r (Fig. 6). Comparison of Fig. 8 ($^{16}O_2$ with 10-CAS-T) and Table 4 ($^{16}O^{17}O$ with 1-CAS-T) indicates that the last function $g_r(r)$ is very similar to the former one (Fig. 8) and is shifted up by about

0.03–0.05; it decreases with long distances a little bit more slowly. The shift is partly connected with different isotope modifications (0.006, Table 4) and mostly-with the CAS extension.

It is interesting to note that the most primitive CAS which includes only six active electrons in four orbitals $\pi_u\pi_g$ (denoted as 0-CAS) produces quite reliable results at the internuclear distance $r = 1.22$ Å, which is close to the r_e value optimized with small CASs. Results are presented in Table 5 together with experimental data obtained from the ESR spectra analysis [13] for different isotope modifications. In [13] the rotational g factor denoted as $g_3 = -g_r$ is not given in (m/M) units, thus it is 1840 times smaller, than the values presented in Table 5. The agreement between 0-CAS-D results and the recalculated experimental data from [13] is surprising (Table 5).

Finally, we have to note that the absolute values of rotational g_r factor in the singlet excited states $a^1\Delta_g$ and $b^1\Sigma_g^+$ calculated at the optimized equilibrium distances are slightly higher than in the ground triplet state: in the 10-CAS-T method (or CAS-II in [40]) the rotational g_r factor have been obtained equal to -0.227 and -0.269 for the a and b states, respectively, which are rather different in comparison with the ground state value -0.21 [40]. The distance dependences $g_r(r)$ are also different. The same trend is found in other active spaces and is in agreement with experimental ESR spectrum of $O_2(a^1\Delta_g)$ obtained by Arrington et al. [50].

3.6. Nuclear spin–rotation coupling constant and NMR shielding

Interaction between nuclear ^{17}O magnetic moment and the internal magnetic field induced by rotational movement arises in the absence of any external fields and produces an additional (behind HFC) splitting of rotational lines, Eq. (2). This interaction is described by the nuclear spin–rotation coupling constant f, Eq. (2), which is closely related to the paramagnetic part of the nuclear magnetic resonance (NMR) shielding constant (chemical shift) and to χ^{para} [36]. The NSRC constant cannot be calculated with the symmetry dependent nuclei. Thus, this constant as well as the molecular g factor have been recalculated in the C_{2v} point group with different active orbital spaces. Results are presented in Tables 3 and 4 (the small 1-CAS) for different isotope modifications and for $^{16}O^{17}O$ molecule, respectively. The NSRC constant, Eq. (2), is often denoted as $f = -M_O$ and produces the energy correction [36]:

$$\Delta E = -I_O M_O K, \tag{13}$$

where I_O represents the spin of the ^{17}O nucleus ($I_O = 5/2$). In oxygen molecule, one has $f = -(1/2)(M_{xx} + M_{yy})$; the electronic (paramagnetic) part of the NSRC constant is [13]:

$$-f = M_{xx} = M_O = -\frac{4eg_O\mu_{NB}}{\hbar cm}\langle r^{-3}\rangle Re\sum_n \frac{|\langle 0|L_x|n\rangle|^2}{E_n - E_0}. \tag{14}$$

For paramagnetic molecule some additional crossing terms occur in the second-order perturbation theory [51], which are neglected here. Comparison of results from different CAS calculations shows that the nuclear spin–rotational constant does not dependent very much on the CAS extension. For example, at $r = 1.22$ Å in different i-CAS with the aug-cc-pVDZ basis set we get for the $^{16}O^{17}O$ molecule the NSRC constant equal to 21.546, 20.991 and 21.502 kHz for $i = 1$, 7 and 10, respectively. The nuclear spin–rotation coupling constants $M(^{17}O)$ for the a and b states are quite similar: at $r = 1.22$ Å they are equal to 21.316 and 21.86 kHz, respectively, at the 1-CAS-D level. The NSRC constants $M(^{17}O)$ for the ground triplet and both singlet excited states increase with r (because of the paramagnetic contribution); the absolute value of the nuclear parts and diamagnetic contribution decrease (Table 4).

Gerber has studied the ESR spectrum of gaseous $^{16}O^{17}O$ molecule and determined the spin–rotation coupling constants $M(^{17}O)$ equal to 55 ± 15 kHz [13]. This is higher than the most accurate value obtained with 10-CAS-T method in the present MCSCF calculations. As follows from Table 4, the NSRC constant strongly increases with internuclear distance; vibrational averaged value for the ground $v = 0$ state is 24.6 kHz. One can anticipate that the calculated NSRC constant is more reliable than that, extracted from the fine structure of the ESR spectrum with high errors. For comparison, the spin–rotation coupling constant for the nitrogen molecule ($^{15}N_2$) is 22.6 kHz [36], for CO molecule ($C^{17}O$) it is 30.4 ± 1.2 kHz [52]. Our MCSCF calculations reproduce these values reasonably well with the 10-CAS-T type of approximation. Probably, the neglected terms [51] in Eq. (14) are important for the ground state oxygen molecule.

Since the ^{17}O NMR spectrum of molecular oxygen has not been measured so far, we present here the results of the NMR shielding constant calculation very shortly. Only temperature independent part of the NMR shielding tensor is calculated. Contributions from HFC and the ensemble averaged spin polarization to σ value cannot be neglected, but their estimation for paramagnetic O_2 molecule with large zero-field splitting is very complicated. At least our results can be applied for high-temperature NMR measurements and for NMR spectrum measured in low-temperature diamagnetic α-oxygen crystal.

The distance dependence of the isotropic part of the σ tensor, $\sigma = (1/3)(\sigma_{zz} + 2\sigma_{xx})$, and of its anisotropy $(\sigma_{zz} - \sigma_{xx})$, calculated by the 10-CAS-T and 11-CAS-T methods are given in Fig. 9; Table 1 presents the isotropic NMR shielding constant, σ, calculated with different CAS-T methods. The NMR shielding constant is a very strong function of the internuclear distance; it changes by a factor of a thousand with r (Fig. 9). The σ value changes sign at $r = 1.18$ Å, near the equilibrium distance; just at the r_e point it has small negative value. The negative paramagnetic contribution to isotropic σ constant (-473.6 ppm) slightly prevails over positive diamagnetic contribution (431.1 ppm): the results are from the 11-CAS-T calculation for $r = 1.2075$ Å.

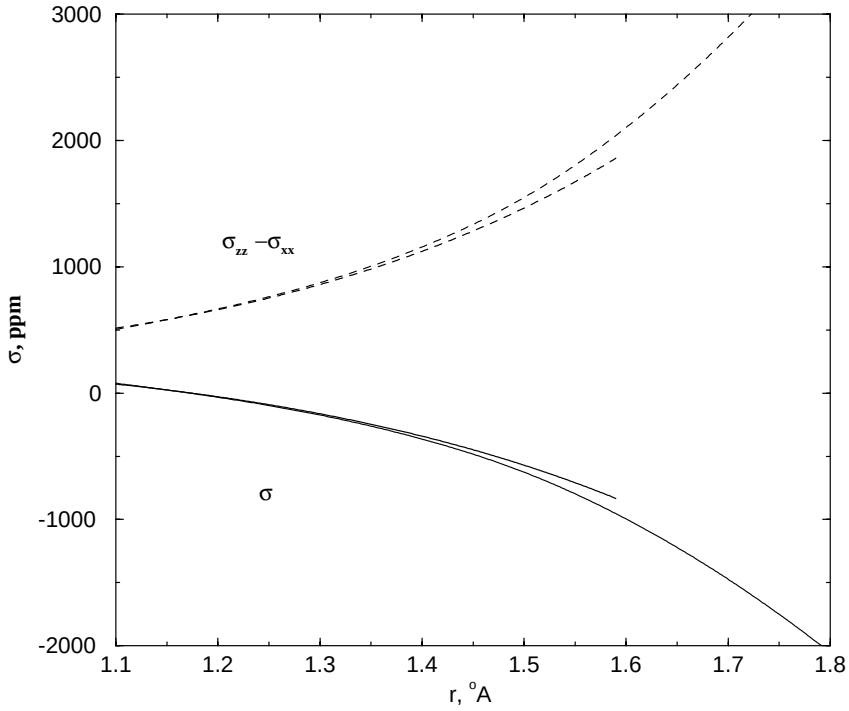

Fig. 9. NMR shielding constant (solid line) and anisotropy of the shielding tensor (dashed line), in ppm, calculated by MCSCF method for the ground $X^3\Sigma_g^-$ state of the $^{17}O_2$ molecule as a function of the internuclear distance r (Å): thin line (10-CAS-T); bold line (11-CAS-T).

Anisotropy at this point is 679.8 ppm. The σ_{xx} component is equal to −269.1 ppm (its diamagnetic and paramagnetic contributions are 441.3 and −710.4 ppm, respectively); the σ_{zz} component consists only from the diamagnetic part and is equal to 410.7 ppm. That it why this delicate balance for the calculated NMR shielding constant is so different in different CAS (Table 1). The σ value calculated with the 11-CAS-T method seems to be quite reliable. For comparison, the isotropic ^{17}O NMR shielding constant in CO molecule is $\sigma = -52.9$ ppm from CCSD(T) calculation; experimental value is -42.3 ± 17.2 ppm (anisotropy is 676 ± 26 ppm) [53]. Our treatment with the 10-CAS-T type of approximation is in a reasonable agreement with this accuracy.

4. Conclusions

The MCSCF calculations with the most accurate 11-CAS-T approximation ((2–4)σ_g(2–4)σ_u(1, 2)π_u(1, 2)π_g active space and aug-cc-pVTZ basis set [35]) which includes a half million configuration state functions in D_{2h} point group produce the following results for the ground state O_2 properties (experimental data are in parentheses): quadrupole moment $Q_{zz} = -0.254ea_0^2$ ($-0.26ea_0^2$ [10]), polarizability $\alpha_{xx} = 8.04a_0^3$ and $\alpha_{zz} = 15.45a_0^3$ (8.16 and $15.45a_0^3$, respectively [9]), temperature-independent part of the isotropic molar magnetic susceptibility $\chi_i = -10.62 \times 10^{-6}\,\mathrm{cm^3\,mol^{-1}}$. Anisotropy, $\chi_{zz} - \chi_{xx} = -2.31$ a.u. $= -10.98 \times 10^{-6}\,\mathrm{cm^3\,mol^{-1}}$, is in excellent agreement with the Cotton–Mouton effect measurement ($-10.66 \times 10^{-6}\,\mathrm{cm^3\,mol^{-1}}$ [11]). It is difficult to measure the diamagnetic (or temperature-independent) part of susceptibility of paramagnetic molecular oxygen [11]; thus, the agreement with the measured anisotropy is a good criterion for a correct magnetizability tensor. The total magnetic susceptibility of molecular oxygen calculated with account of the electronic g factor in the same 11-CAS-T method ($g_{xx} = 2.0052$) is equal to $3.42 \times 10^{-3}\,\mathrm{cm^3\,mol^{-1}}$ at 293 K, which is in a good agreement with the commonly accepted value ($3.45 \times 10^{-3}\,\mathrm{cm^3\,mol^{-1}}$ [49]). Thus, the reported small deviations from the Curie's law for gaseous molecular oxygen might be ascribed to measurement errors [47].

A good description of the temperature-independent susceptibility provides also a reliable interpretation of the rotational g_r factor. The value calculated with the 11-CAS-T approximation, $g_r = -0.23\,(m/M) = -0.000125$, is in excellent agreement with the microwave spectral data ($g_r = -0.000128$ [46]). A reasonable agreement with the ESR experiment [13] is obtained for the rotational g_r factor of all possible isotope modifications (Table 5). Calculations show that the g_r factor is a strong function of the internuclear distance which has a maximum near the equilibrium (Fig. 8).

The following fine structure constants, depending on the ^{17}O nucleus, are also calculated. The nuclear quadrupole coupling constant of the ^{17}O nucleus, estimated as

$e^2qQ/h = -8.31$ MHz, is in a good agreement with the ESR spectrum of gaseous $^{16}O^{17}O$ (-8.42 ± 0.18) MHz [13]. The absolute value of the negative NQC constant strongly increases with r in the vicinity of the equilibrium (Fig. 4), thus it is quite different for higher rotational and vibrational states. The nuclear spin–rotation coupling constant is calculated in the 10-CAS-T approximation to be equal to 24.6 kHz, which is smaller than the NSRC constant obtained from the ESR fine structure measurement (55 ± 15 kHz [13]). Comparison with other molecules provides additional arguments in favour of the theoretical prediction. The NSRC constant strongly increases with r. The isotropic NMR shielding constant predicted to be equal to -42.5 ppm with very high anisotropy parameter (679.8 ppm). The London atomic orbitals have been used to ensure gauge-origin independent results in calculations of these magnetic properties. The hyperfine coupling constants calculated by UHF method ($b = -101$ MHz and $c = 140$ MHz) are in agreement with previous studies [14]. A new finding is that the spin density at the nucleus, $\psi^2(0)$, is a strongly descending function of the internuclear distance (Fig. 2). It is well known that the commonly used contracted Gaussian basis sets do not describe properly the spin density near the nucleus [37]. Thus, it is not a surprise that the Slater-type basis set, being worse for many molecular properties, gives better results for the $\psi^2(0)$ value than the splitted GTO basis. The HFC constant is the only property which has been calculated in present MCSCF study by uncontracted basis set with additional five tight s functions in order to reproduce the s-type behavior in the vicinity of the nucleus.

Such parameters and properties as quadrupole moment (Fig. 3), magnetizability (Fig. 6) and the NMR shielding tensor (Fig. 8), being strongly dependent on r, change their sign in the vicinity of the equilibrium distance r_e. Thus, the vibrational averaged (observed) values are rather small and very sensitive to the accuracy of calculation. The potential energy curves of eight excited states calculated by the MCSCF response method with the 10-CAS-T approach (Fig. 1) are in agreement with other studies [21,26]. This gives additional support to the accuracy of the calculated ground state properties of the O_2 molecule.

Acknowledgements

This work was supported by the Swedish Royal Academy of Science.

References

[1] D. Sawyer, Oxygen Chemistry, Oxford University, New York, 1991.
[2] B. Minaev, Science dissertation, Chem. Phys. Institute, Moscow, 1983.
[3] B. Minaev, Russ. J. Struct. Chem. 23 (1982) 170.
[4] B. Minaev, Sov. J. Chem. Phys. 3 (1985) 1533.
[5] R. Prabhakar, P. Siegbahn, B. Minaev, H. Ågren, J. Phys. Chem. B 106 (2002) 3742.
[6] B. Minaev, Opt. Spectrosc. (USSR) 58 (1985) 1238.
[7] P. Luchette, R. Prosser, C. Sanders, J. Am. Chem. Soc. 124 (2002) 1778.
[8] B. Minaev, H. Ågren, Coll. Szechoslovak Chem. Commun. 60 (1995) 339.
[9] D. Spelsberg, W. Meyer, J. Chem. Phys. 101 (1994) 1282.
[10] E. Cohen, G. Birnbaum, J. Chem. Phys. 66 (1977) 2443.
[11] H. Kling, E. Dreier, W. Huttner, J. Chem. Phys. 78 (1983) 4309.
[12] M. Tinkham, M. Strandberg, Phys. Rev. 97 (1955) 951.
[13] P. Gerber, Helv. Phys. Acta 45 (1972) 655.
[14] S. Miller, C. Townes, M. Kotani, Phys. Rev. 90 (1953) 542.
[15] C. Townes, A. Schawlow, Microwave Spectroscopy, McGraw-Hill, New York, 1955.
[16] M. Tinkham, M. Strandberg, Phys. Rev. 97 (1955) 937.
[17] R. Frosch, H. Foley, Phys. Rev. 88 (1952) 1337.
[18] M. Kotani, Y. Mizuno, K. Kayama, E. Ishiguro, J. Phys. Soc. Jpn. 12 (1957) 707.
[19] W. Rijks, M. van Heeringen, P. Wormer, J. Chem. Phys. 90 (1989) 6501.
[20] Y. Luo, H. Ågren, B. Minaev, P. Jorgensen, J. Mol. Struct. (TEOCHEM) 336 (1995) 61.
[21] K. Huber, G. Herzberg, Molecular Spectra and Molecular Structure. Constants of Diatomic Molecules, vol. 4, Van Nostrand Reinhold, New York, 1979.
[22] B. Minaev, Opt. Spectrosc. (USSR) 45 (1978) 936.
[23] B. Minaev, Izv. Vyssh. Uchebn. Zaved. Fiz. 9 (1978) 115.
[24] B. Minaev, J. Mol. Struct. (THEOCHEM) 183 (1989) 207.
[25] S. Langhoff, C. Kern, in: H. Schaeffer (Ed.), Methods of Electronic Structure Theory, vol. 4, Plenum Press, New York, 1977.
[26] B. Hess, C. Marian, S. Peyerimhoff, in: D.R. Yarkoney (Ed.), Modern Electronic Structure Theory. Part I, World Scientific, Singapore, 1995, p. 152.
[27] B.M.O. Vahtras, O.L.H. Ågren, K. Ruud, Chem. Phys. 279 (2002) 133.
[28] H. Ågren, O. Vahtras, B. Minaev, Adv. Quant. Chem. 27 (1996) 71.
[29] O. Vahtras, B. Minaev, H. Ågren, Chem. Phys. Lett. 281 (1997) 186.
[30] M. Engstrom, B. Minaev, O. Vahtras, H. Ågren, Chem. Phys. 237 (1998) 149.
[31] H.J.A. Jensen, P. Jørgensen, T. Helgaker, J. Olsen, Chem. Phys. Lett. 154 (1989) 380.
[32] B. Minaev, Phys. Chem. Chem. Phys. 1 (1999) 3403.
[33] B. Minaev, Chem. Phys. 252 (2000) 25.
[34] B. Minaev, O. Vahtras, H. Ågren, Chem. Phys. 208 (1996) 299.
[35] D. Woon, T. Dunning, J. Chem. Phys. 98 (1993) 1358.
[36] J. Gauss, K. Ruud, T. Helgaker, J. Chem. Phys. 105 (1996) 2804.
[37] B. Fernandez, P. Jorgensen, J. Simons, J. Chem. Phys. 98 (1993) 7012.
[38] T. Helgaker, H.J.A. Jensen, P. Jørgensen, J. Olsen, K. Ruud, H. Ågren, T. Andersen, K. L. Bak, V. Bakken, O. Christiansen, et al., Dalton Release 1.0, An Electronic Structure Program, 1997.
[39] M. Schmidt, K. Baldridge, J. Boats, S. Elbert, M. Gordon, J.H. Jensen, S. Koseki, N. Matsunaga, K. Nguyen, S. Su, et al., J. Comput. Chem. 14 (1993) 1347.
[40] B. Minaev, V. Minaeva, Phys. Chem. Chem. Phys. 3 (2001) 720.
[41] S. Miller, C. Townes, Phys. Rev. 90 (1953) 537.
[42] T. Dunning, P. Hay, in: H. Schaeffer (Ed.), Methods of Electronic Structure Theory, vol. 3, Plenum Press, New York, 1977.
[43] J. Hirschfelder, C. Curtiss, R. Bird, Molecular Theory of Gases and Liquids, Wiley, New York, 1954.
[44] A. Buckingham, R. Disch, D. Dunmur, J. Am. Chem. Soc. 90 (1968) 3104.
[45] D. Spelsberg, W. Meyer, J. Chem. Phys. 109 (1998) 9802.
[46] K. Evenson, M. Mizushima, Phys. Rev. (1972) 2197.

[47] J. van Vleck, The Theory of Electric and Magnetic Susceptibilities, Oxford University Press, 1932, p. 266.
[48] K. Ruud, T. Helgaker, K. Bak, P. Jørgensen, J. Olsen, Chem. Phys. 195 (1995) 157.
[49] D. Lide, CRC Handbook of Chemistry and Physics, 73rd ed., CRC Press, Boca Raton, FL, 1993.
[50] J.C.A. Arrington, A. Falick, R. Myers, J. Chem. Phys. 55 (1971) 909.
[51] B. Minaev, O. Loboda, Z. Rinkevicius, O. Vahtras, H. Ågren, Mol. Phys 102 (2003) 1.
[52] S. Freilich, K. Peters, J. Am. Chem. Soc. 103 (1981) 6255.
[53] J. Gauss, J. Stanton, J. Chem. Phys. 104 (1996) 2574.